

This is an Open Access document downloaded from ORCA, Cardiff University's institutional repository: <https://orca.cardiff.ac.uk/id/eprint/126031/>

This is the author's version of a work that was submitted to / accepted for publication.

Citation for final published version:

Dai, Xiaoxia, Wang, Xinwei, Long, Yunpeng, Pattison, Samuel, Lu, Yunhao, Morgan, David John , Taylor, Stuart H. , Carter, James H., Hutchings, Graham J. , Wu, Zhongbiao and Weng, Xiaole 2019. Efficient elimination of chlorinated organics on a phosphoric acid modified CeO₂ catalyst: a hydrolytic destruction route. *Environmental Science and Technology* 53 (21) , pp. 12697-12705. 10.1021/acs.est.9b05088

Publishers page: <http://dx.doi.org/10.1021/acs.est.9b05088>

Please note:

Changes made as a result of publishing processes such as copy-editing, formatting and page numbers may not be reflected in this version. For the definitive version of this publication, please refer to the published source. You are advised to consult the publisher's version if you wish to cite this paper.

This version is being made available in accordance with publisher policies. See <http://orca.cf.ac.uk/policies.html> for usage policies. Copyright and moral rights for publications made available in ORCA are retained by the copyright holders.



Supporting Information

Efficient Elimination of Chlorinated Organics on A Phosphoric Acid Modified CeO₂ Catalyst: A Hydrolytic Destruction Route

Xiaoxia Dai, Xinwei Wang, Samuel Pattison, Yunhao Lu, David J. Morgan, Stuart H. Taylor,

James H. Carter*, Graham J. Hutchings, Xiaole Weng*, Zhongbiao Wu

Number of Pages: 5

Number of Figures: 4

Number of Tables: 3

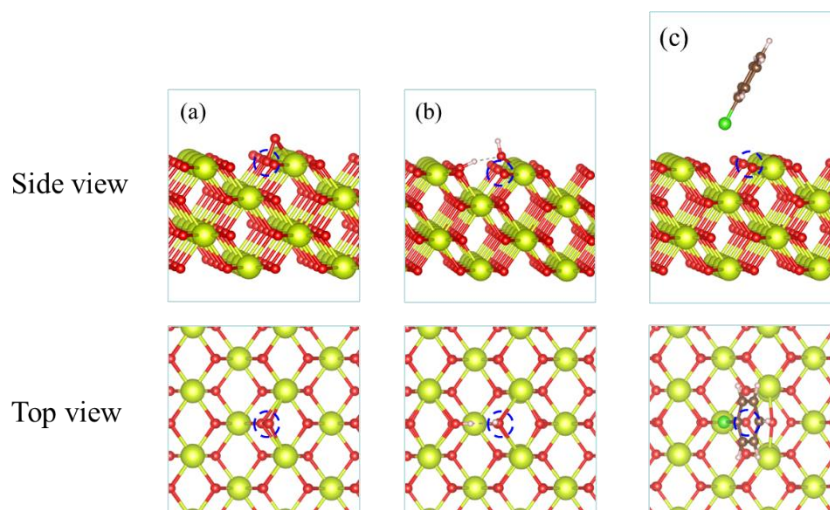


Figure S1. Optimized model of CeO₂ (110) with oxygen vacancy. The models were constructed by removing single oxygen atom from CeO₂(110) supercell to introduce oxygen vacancies. During geometry optimization, the atoms in the top two layers of CeO₂ slab were allowed to relax while atoms in the bottom two layers were fixed in their optimized bulk positions.

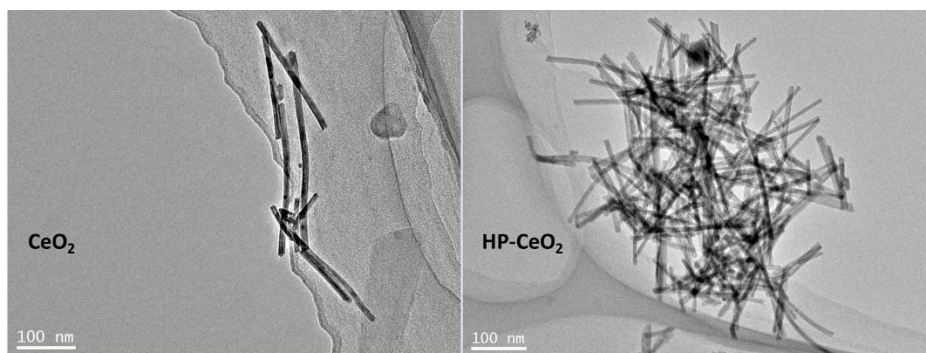


Figure S2. TEM images of CeO₂ and HP-CeO₂

Table S1. Physical properties of HP-CeO₂ and CeO₂

| sample | p loading | | surface area (m ² g ⁻¹) | lattice parameter (Å) | Ce ³⁺ /Ce _{total} ^a |
|---------------------------|-------------------------|---------------------|---|--------------------------|--|
| | (mmol g ⁻¹) | (nm ⁻²) | | | |
| CeO₂ | 0 | 0 | 96 | 5.411 | 29% |
| HP-CeO₂ | 0.21 | 1.18 | 108 | 5.413 | 26% |

Note: (a) caculated from XPS results

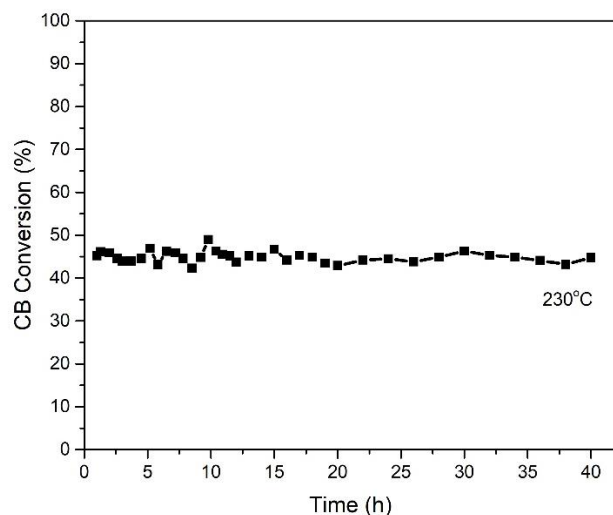


Figure S3. Stability test of CB oxidation over HP-CeO₂ at 230 °C. Reaction condition: GHSV at 10,000 mL/(g h), chlorobenzene at ca. 500 ppm, H₂O at 5000 ppm, N₂ flow rate at ca. 145 mL/min, O₂ flow rate at ca. 15 mL/min.

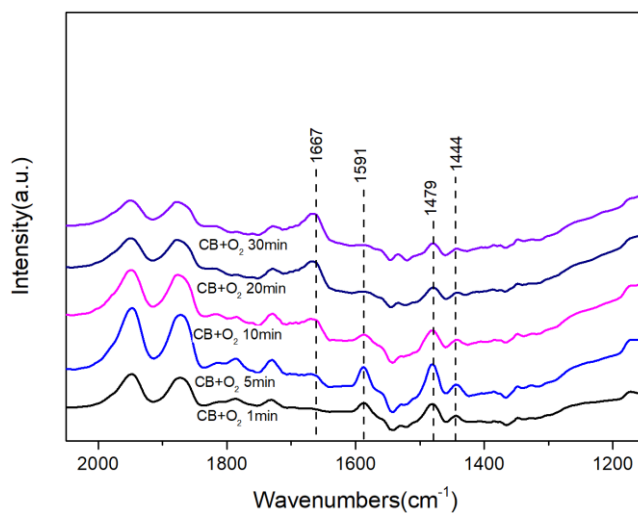


Figure S4. *in-situ* FTIR spectra of CB oxidation at 150 °C over CeO₂ catalyst in dry condition.

Table S2. Adsorption energies on various active sites

| Species | Adsorption energy (eV) |
|---|------------------------|
| O ₂ /O _{vac} | 2.20 |
| H ₂ O/O _{vac} | 1.57 |
| O ₂ +H ₂ O/O _{vac} | 2.82 |
| C ₆ H ₅ Cl/O _{vac} | 0.39 |
| C ₆ H ₅ Cl+O ₂ /O _{vac} | 2.37 |

| | |
|--|-------|
| C ₆ H ₅ Cl+H ₂ O/O _{vac} | 1.21 |
| O ₂ /Ce | 0.20 |
| H ₂ O/Ce | 0.62 |
| O ₂ +H ₂ O/Ce | 0.72 |
| C ₆ H ₅ Cl/Ce | 0.48 |
| C ₆ H ₅ Cl+H ₂ O/Ce | 1.81 |
| O ₂ /P group | -1.59 |
| H ₂ O/P group | 0.63 |
| O ₂ +H ₂ O/P group | -0.94 |
| C ₆ H ₅ Cl/P group | 0.50 |
| C ₆ H ₅ Cl+O ₂ /P group | -0.56 |
| C ₆ H ₅ Cl+H ₂ O/P group | 2.77 |
| HCl/P group | 0.74 |
| C ₆ H ₅ OH/P group | 0.76 |

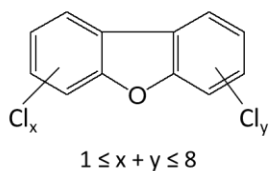
Table S3. Ingredients of 17 toxic dioxins in the off-gas of CeO₂ and HP-CeO₂ at 250 °C test with H₂O stream

| Compound | Detection limit (pg) | TEF | CeO ₂ | | HP-Ce | |
|--------------------|----------------------|-----|------------------|----------------------------|-----------|----------------------------|
| | | | Cout (pg) | I-TEQ (ng/m ³) | Cout (pg) | I-TEQ (ng/m ³) |
| 2378TCDD | 0.5627 | 1 | <0.5627 | ND | <0.5627 | ND |
| 12378PeCDD | 0.6234 | 0.5 | <0.6234 | ND | <0.6234 | ND |
| 123478HxCDD | 0.6574 | 0.1 | <0.6574 | ND | <0.6574 | ND |

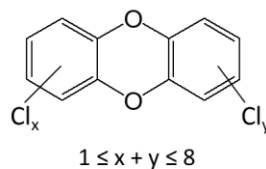
| | | | | | | |
|---------------------|--------|-------|---------|----------|---------|----|
| 123678HxCDD | 0.625 | 0.1 | 1.4879 | 0.00155 | <0.625 | ND |
| 123789HxCDD | 0.6931 | 0.1 | <0.6931 | ND | <0.6931 | ND |
| 1234678HpCDD | 0.5632 | 0.01 | 6.2856 | 0.000655 | <0.5632 | ND |
| OCDD | 0.7633 | 0.001 | 4.2767 | 4.45E-05 | <0.7633 | ND |
| 2378TCDF | 0.4675 | 0.1 | 0.9775 | 0.001018 | <0.4675 | ND |
| 12378PeCDF | 0.642 | 0.05 | 1.2645 | 0.000659 | <0.642 | ND |
| 23478PeCDF | 0.6132 | 0.5 | 1.04855 | 0.005461 | <0.6132 | ND |
| 123478HxCDF | 0.6015 | 0.1 | 2.3201 | 0.002417 | <0.6015 | ND |
| 123678HxCDF | 0.6329 | 0.1 | 2.5632 | 0.00267 | <0.6329 | ND |
| 123789HxCDF | 0.6512 | 0.1 | 0.57475 | 0.000599 | <0.6512 | ND |
| 234678HxCDF | 0.6877 | 0.1 | 2.3671 | 0.002466 | <0.6877 | ND |
| 1234678HpCDF | 0.7022 | 0.01 | 5.3266 | 0.000555 | <0.7022 | ND |
| 1234789HpCDF | 0.6934 | 0.01 | <0.6934 | ND | <0.6934 | ND |
| OCDF | 0.7142 | 0.001 | 3.3276 | 3.47E-05 | <0.7142 | ND |
| Total | | | | 0.01813 | | ND |

Note: (1) CDD/CDF: chlorinated dibenzo-*p*-dioxin/dibenzofuran, structural formula represents as Fig S10 ; (2) ND: not detectable; (3) I-TEQ = Cout × TEF; (4) TEF: Toxic Equivalent Factors, toxic factors relative to the most toxic congener, 2,3,7,8-tetrachlorodibenzo-dioxin; (5) I-TEQ: International Toxicity Equivalence Quotient, the weighted value of the concentrations of 17 PCDD and PCDF congeners with chlorine in the 2, 3, 7 and 8 positions on the dibenzo skeleton, weighted according their Toxic Equivalent Factors (TEF) relative to the most toxic congener, 2,3,7,8-tetrachlorodibenzo-dioxin.

Polychlorinated dibenzofurans



Polychlorinated dibenzo-*p*-dioxins



Structure diagrams of chlorinated dibenzo-*p*-dioxin/dibenzofuran